บทความวิจัย

HYPERBRANCHED POLY (L-LACTIDE) BY USING POLYGLYCIDOL FOR GREEN ENVIRONMENT

Nichakorn Pathumrangsan*
Department of General Science, Faculty of Science and Technology,
Muban Chom Bueng Rajabhat University, 70150, Thailand

*E-mail: nichakornpat@mcru.ac.th

Received: 03-12-2021
Revised: 13-08-2022
Accepted: 23-08-2022

ABSTRACT

Hyperbranched poly(L-lactide) (*hb*-PLLA)s for green environment were synthesized by ring-opening polymerization of L-lactide (LLA) using polyglycidol (PG) as an initiator. *hb*-PLLAs were blended with linear PLLA (l-PLLA) by varying the LLA branch content. Thermal, Mechanical and rheological properties, and optical transparency of *hb*-PLLAs and their blends with l-PLLA were investigated. All l-PLLA/*hb*-PLLAs blends showed slightly changes of T_g values, whereas the T_m was significantly unchanged. A single T_g was observed in all blends, indicating a completely miscible system. All blends exhibited an increase in crystallinity, as the branch structure acted as nucleating agent for crystallization of l-PLLA. Viscosity of the blends was decreased with the addition of l-PLLA. This provides easy processing conditions. The blends also showed high optical transparency, comparable to neat l-PLLA. Given these properties and their biocompatibility, the blends can be used in biomedical applications.

Keywords: Branch structure; Blended Polylactide; Polylactide; Polyglycidol

Introduction

Nowadays, polylactide (PLA) has received much attention, due to serious environmental problems on plastic wastes. PLA is one of well-known degradable polymers, which provides many good properties, such as high mechanical strength, transparency, and biocompatibility (Ajioka et al., 1995; Tuominen et al., 2002; Fan et al., 2004). PLAs are widely used in many applications, especially in biomedical field (Uurto et al., 2005; Ormiston and Serruys, 2009; Rasal, Janorkar and Hirt, 2010)

However, PLA-based materials possess certain disadvantages which limit their use in some applications, e.g., brittleness, and difficulty in controlling degradation rates. Many approaches

have been performed to overcome these drawbacks, such as stereocomplexation, introduction of branch-structured PLA, and blending with other polymers. Among these, introducing of branch structures into PLA matrix is a promising method to solve these problems. Polymers with branch architectures typically have lower glass transition temperature (T_g) and melt viscosity than their linear counterparts of similar molecular weight. Moreover, branch length is an important parameter that affects the viscoelasticity of fluidity range and crystallinity (Ouchi, Ichimura and Ohya ,2006). The use of various hydrophilic cores have been reported in preparation of branched PLA copolymers, such as, poly(ethylene glycol) (PEG), poly(ethylene oxide) (PEO) (Choi, Bae and Kim, 1998; Pistel et al., 1999; Salaam, Dean and Bray, 2006), poly(amido amine) (PAMAM) (Cai et al., 2003), and polyglycidol (PG) (Ouchi, Ichimura and Ohya ,2006; Kainthan et al. 2006; Cabral et al., 2018; Atkinson and Vyazovkin 2012; Michalski et al., 2019)

In this study, hyper branched PLLA (*hb*-PLLA) is developed for intended use in biomedical applications. PG is chosen as a hydrophilic core because of its multi-functionality, which can be used as a macro-initiator for polymerization of PLA, and its biocompatibility (Kainthan et al. 2006). Ring-opening polymerization in bulk is employed (Xu et al.,2021). The resulting *hb*-PLLAs is blended with linear PLLA (*l*-PLLA) to optimize its physical and rheological properties.

Materials

L-Lactide (LLA) and tin octoate ($Sn(Oct)_2$) were purchased from Wako (Japan). Linear PLLA (l-PLLA) (MW = 178,000 g/mol) was supplied by PURAC (Netherland). PG macro-initiator was synthesized according to a methodology reported earlier (Petchsuk et al.,2014). Ethyl acetate, chloroform, ethanol and toluene solvents were purchased from Lab Scan (Thailand).

Methods

1. Synthesis of *hb*-PLLAs

Hyper branched PLLAs (*hb*-PLLAs) were synthesized by ring-opening polymerization, using PG and $Sn(Oct)_2$ as a macro-initiator and catalyst. Polymerization temperature and time for *hb*-PLLAs are 120 °C and 24 h. The weight ratio of PG to l-LA was varied 1:10, 1:20, 1:50 and 1:100. The products were purified by dissolving in chloroform and precipitated in mixing solvent (ethanol/hexane), and then dried them under vacuum at 50 °C for 2 days.

2. Blend of l-PLLA and *hb*-PLLAs

The synthesized products were blended with a l-PLLA by melt mixing in an internal mixer (MIX105-D40L50) using a rotor speed of 50 rpm and blending time and temperature of 20 min and 170 °C. Blend ratios of *hb*-PLLAs to l-PLLA of 5/95, 10/90, 15/85, and 20/80 were employed. The blended samples were then presses into a film form by a compression machine (PR2D-W300L300 HD-WCL).

3. Characterizations

Chemical structures of *hb*-PLLA were characterized on an AVEN-CEIII 500 MHz digital Nuclear Magnetic Resonance spectrometer (NMR) (AV-500, Bruker Biospin), using $CDCl_3$ solvent. For thermal properties, *hb*-PLLAs and their blended samples were measured by differential scanning calorimetry (DSC) (DSC822e Mettler Toledo) at a heating/cooling rate of 20 °C/min. All specimens were heated to 200 °C (first scan) to erase their thermal history, and then cooled to -20 °C. The samples were then heated from -20 to 220 °C.

Tensile properties of blends (PLLA/*hb*-PLLA) were measured on a universal testing machine with a crosshead speed of 50 mm/min and a 100 N load cell (Instron model 55R4502, Instron Corp., USA). The specimens were cut into rectangular shape with 50 mm gauge length and 15 mm width, according to ASTM D882. The five specimens were tested on each tensile test.

Rheological properties, in terms of complex viscosity (η^*) of the blends were measured on a strain-controlled rheometer (ARES, TA Inc., New Castle, USA). Samples were prepared into a disc form with a diameter of 25 mm and 1 mm thickness. The strain amplitude was fixed at 0.5%. The samples were scanned from 140 – 200 °C with a heating rate of 10 °C/min at a frequency of 1 rad/s.

UV/VIS spectroscopy was used to measure the transparency of blended PLLA films. UV/VIS measurements were obtained using a Perkin-Elmer UV/VIS Lambda 12 Spectrophotometer. The blended PLLA films were loaded in a quartz flow cell and were measured in scanning mode (400-600 nm) at room temperature.

Results and Discussions

1. Chemical structure and properties of *hb*-PLLAs

The proposed structure and ^{1}H-NMR spectra of the synthesized branched PLLA were shown in Figure 1. The peaks d, e and f (δ = 1.5, 5.1 and 4.3 ppm) were assigned to methyl, methylene and methine protons at end groups of lactate units. The signals a and b (δ = 3.4 – 3.6 ppm) indicated the methine and methylene proton of PG. The peak c and f overlapped in ^{1}H-NMR spectra of *hb*-PLLA. The integral ratio of the signal at 5.1 and 4.3 affected to average l-LA length/ branch (l-LA). The values of l-LA/PG composition in chain were calculated from the integral ratio of the signal at 3.4 - 3.6 and 5.1 ppm.

l-LA/PG values of the branched PLLA and the average l-LA length evaluated from ^{1}H-NMR spectrum increased with an increase in the feed ratio, as summarized in Table 1. Therefore, we can control length of PLLA chain by varying the feed ratios. (The code, e.g. *hb*-PLLA101, means PLLA that synthesized to have many branch on structure and 101 is weight ratio of LLA per PG.

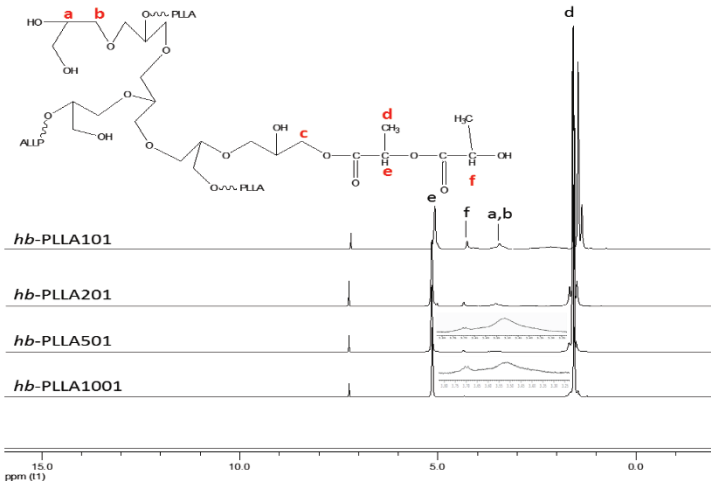

Figure 1 Chemical structures and ^{1}H-NMR spectra of *hb*-PLLAs synthesized from different feed ratios: *hb*-PLLA101, *hb*-PLLA201, *hb*-PLLA501, and *hb*-PLLA1001

Table 1 Evaluation of LLA/PG compositions and arm length of LLA sequences.

	(l-LA)/PG *composition*		l-LA$_n^a$ *composition*
	in feed	in chain	
***hb*-PLLA101**	10/1	22/1	13
***hb*-PLLA201**	20/1	29/1	16
***hb*-PLLA501**	50/1	65/1	38
***hb*-PLLA1001**	100/1	187/1	71

[a] Calculated from integral ratios of e/f, l-LAn = average l-LA length/branch

2. Thermal properties of hb-PLLAs and their blends

DSC thermograms of *hb*-PLLAs showed glass transition temperature (T_g) ranging 48-63 °C. However, *hb*-PLLA 501 and 1001 showed the melting temperature (T_m) at 147 and 163 °C, respectively. T_g showed in Table 2 in table 2 showed that t_g was increased when the chain length of branch PLLA due to the chain mobility. For T_m, long l-LA sequences (*hb*-PLLA 501 and 1001) were able to form the crystalline domains. In general, polymer chain can pack together and crystallize when the polymer structure is regular and symmetrical. Chain end either produce imperfect lattice in crystallinities or are not incorporate into the crystalline regions resulting in a lower T_m.

Table 2 Thermal properties of neat l-PLLA and *hb*-PLLAs with different structures.

Sample	T_g [°C]	T_m [°C]	ΔH_m [J/g]	T_c [°C]	ΔH_c [J/g]
***l*-PLLA**	63	153	0.2		
***hb*-PLLA101**	48	-	-	-	-
***hb*-PLLA201**	47	-	-	-	-
***hb*-PLLA501**	57	147	36.3	121	29.3
***hb*-PLLA1001**	61	163	41.0	121	34.9

Effects of branched structures in terms of arm length and composition of the branched structure component on thermal properties of the l-PLLA/*hb*-PLLA blends are investigated. Results in Table 3 show that a single T_g is observed in all blends, indicating miscible blends, and also reveal 2 trends; (i) short branched PLLA decrease T_g and (ii) long branched PLLA increase T_g of blends. As these short branched PLLAs are miscible with PLLA matrix, the mobility of the branched structure induces the movement of PLLA main component. This results are similar to these reported by Phuphuak and Chirachanchai (2013) that short branching chains PLLA reduce T_g of PLLA by acting as a plasticizer. The degree of reduction also increases with the content of the branched structures. In contrast, T_g of blends containing long branched PLLA slightly increases, since long branched PLLA reduce free volume for chain-end movement and perform chain entanglement with PLLA matrix. Tm of blends are significantly unchanged with addition of branched PLLA. This exhibits that high content of branched PLLA do not result in the increasing of crystal structure. Nevertheless, crystallinity of all blends is higher than neat PLLA, as branched PLLA acts as a nucleating agent inducing crystallization. This result conforms to the report of Shibata et al. (2006) and Rosli et al. (2021).

Table 3 Thermal properties (2nd heating scan) of l-PLLA/*hb*-PLLA101 blends containing various blend ratios

l-PLLA/*hb*-PLLA	T_g [°C]	T_{cc} [°C]	T_m [°C]	ΔH_{cc} [J/g]	ΔH_m [J/g]	χ_c(%)
100/0	63	-	153	-	0.2	0.2
95/5	62	128	156	20	20	21.5
90/10	61	131	156	15	15	16.1
85/15	60	132	155	15	15	16.1
80/20	59	135	155	4	4	4.3

The degree of crystallinity (χ_c) of PLLA was calculated using the following equation (1)

$$\chi_c = \frac{\Delta H_m}{\Delta H^\circ_m} \times 100 \quad (1)$$

Where: ΔH_m Hm is the heat of fusion of the samples

ΔH°_m Hom is the heat of fusion of completely crystallized PLA, i.e. 93 J g-1.

Effect of PLLA arm length of *hb*-PLLA on thermal properties of the l-PLLA/*hb*-PLLA blends were considered by varying branch chain length. When the branch length increases, an increase T_g and T_m is observed in all blends, due to their lower mobility and existent of crystal structure. Cold crystallization of neat PLLA is not observed, because of the presence of some additives from commercial processing. The addition of *hb*-PLLA, however, induces the formation of crystalline domains. ΔH_{cc} of the blends containing long branched PLLA is lower than their ΔH_m. This melt crystallization, as these longer PLLA sequence can induce the melt crystallization more effectively, i.e. at higher rate than the cooling rate of DSC experiment. However, crystallization is not complete, when blend is reheated higher than T_g, further chain rearrangements take place during cold crystallization.

Effect of PLLA arm length of *hb*-PLLA on thermal properties of the l-PLLA/*hb*-PLLA blends were considered by varying branch chain length. When the branch length increases, an increase T_g and T_m is observed in all blends, due to their lower mobility and existent of crystal structure. Cold crystallization of neat PLLA is not observed, because of the presence of some additives from commercial processing. The addition of *hb*-PLLA, however, induces the formation of crystalline domains. ΔH_{cc} of the blends containing long branched PLLA is lower than their ΔH_m. This melt crystallization, as these longer PLLA sequence can induce the melt crystallization more effectively, i.e.

at higher rate than the cooling rate of DSC experiment. However, crystallization is not complete, when blend is reheated higher than T_g, further chain rearrangements take place during cold crystallization.

Table 4 Thermal properties (2nd heating scan) of PLLA and *l*-PLLA/*hb*-PLLA (90/10) blends containing various length of *hb*-PLLAs

Blend component	T_g [°C]	T_{cc} [°C]	T_m [°C]	ΔH_{cc} [J/g]	ΔH_m [J/g]	χ_c(%)
Neat PLLA	63	-	153	-	0.2	0.2
l-PLLA/*hb*-PLLA101	61	131	156	15	15	16.1
l-PLLA/*hb*-PLLA201	61	125	153	24	25	26.9
l-PLLA/*hb*-PLLA501	64	132	154	12	11	11.8
l-PLLA/*hb*-PLLA1001	62	125	155	21	25	26.9

3. Mechanical properties

The mechanical properties of polymeric material that are most frequently evaluated are the tensile strength, Young's modulus, elongation at break, and toughness. A typical goal of enhancement of PLA properties is to increase the elongation at break and toughness. Results on neat PLLA and all blends (l-PLLA/*hb*-PLLA101) as a function of the blend ratios are shown in Table 5, whereas results on effect of the branched chain length are shown in Table 6. The addition of short branched PLLA leads to a decline in mechanical properties of the blends, because branch chain length does not optimize into enhance mechanical properties of PLLA. For long branched PLLA, mechanical properties of the blends slightly change with the increase in the blend compositions. Significant improvement in the properties are observed in blends containing long-branched structure at an optimum composition, e.g. at 90/10 for PLLA/hb-PLLA501 and 95/5 for PLLA/*hb*-PLLA1001, respectively. Toughness of PLLA/*hb*-PLLA501 (90/10) shows the highest value and other mechanical properties; tensile strength, Young's modulus and elongation at break. This reflect an influence of an optimum blend ratio on the improvement of blends mechanical properties.

Table 5 Mechanical properties of l-PLLA/*hb*-PLLA101 blends, as a function of blend ratios

Blend ratios	Tensile strength [MPa]	Young's modulus [MPa]	Elongation at break [%]	Toughness [x 10^5 mJ/mm^3]
100/0	60.5 ± 2.0	2609 ± 62	2.8 ± 0.1	9.8 ± 0.3
95/5	52.2 ± 1.4	2474 ± 45	2.5 ± 0.2	8.4 ± 1.7
90/10	49.3 ± 1.3	2500 ± 31	2.3 ± 0.1	7.6 ± 0.9
85/15	42.9 ± 1.3	2348 ± 36	2.2 ± 0.2	5.9 ± 1.1
80/20	26.0 ± 2.0	2508 ± 68	1.1 ± 0.1	1.5 ± 0.2

Table 6 Mechanical properties of l-PLLA/*hb*-PLLA (90/10) blends consisting of *hb*-PLLA different chain lengths

Blend component	Tensile strength [MPa]	Young's modulus [MPa]	Elongation at break [%]	Toughness [x 10^5 mJ/mm^3]
Neat PLLA	60.5 ± 2.0	2609 ± 62	2.8 ± 0.1	9.8 ± 0.3
l-PLLA/*hb*-PLLA101	49.3 ± 1.3	2500 ± 31	2.3 ± 0.1	7.6 ± 0.9
l-PLLA/*hb*-PLLA201	52.6 ± 0.4	2535 ± 66	2.4 ± 0.1	8.1 ± 0.9
l-PLLA/*hb*-PLLA501	57.3 ± 1.2	2496 ± 50	2.8 ± 0.1	11.3 ± 2.0
l-PLLA/*hb*-PLLA1001	53.6 ± 2.1	2731 ± 69	2.3 ± 0.1	7.2 ± 0.8

4. Rheological properties of l-PLLA/hb-PLLA blends

Complex viscosity (η^*) of l-PLLA/*hb*-PLLA blends consisting of different *hb*-PLLAs at the blend composition of 90/10 wt. is measured, as a function of temperature at a fixed strain of 0.5%. The results are shown in Figure 2. At the temperatures below Tm of the samples, blends containing short LLA branches exhibit low η^* values, as this acts as a plasticizer in the l-PLLA matrix. This is in accord with our previous results (Petchsuk et al., 2014). In contrast, blends consisting of long LLA branches, especially *hb*-PLLA501, show an increase in the values, compared to neat l-PLLA, indicating strong interaction between the blend components, likely due to higher degree of chain entanglements. However, at the temperatures range higher than T_m, where the samples are in melt state, the samples is observed in an opposite trend. This is likely due to the contribution of the

branched structure with longer arm lengths. The insight into this property is essential in fabrication of PLLA products for use in biomedical applications.

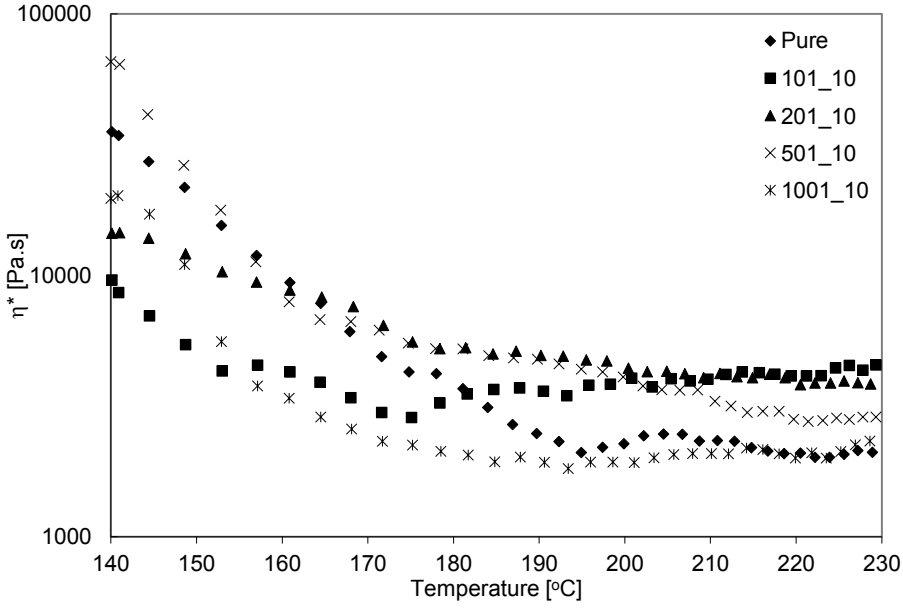

Figure 2 Temperature dependence of complex viscosity (η*) of *l*-PLLA/*hb*-PLLA blends containing different *hb*-PLLAs.

5. Optical transparency of blends

To examine the effect of branched PLLA on the optical transparency of the blends, blend's films were made by hot press with a thickness ranging from 0.14 – 0.20 mm, and absorbance in visible region is measured. Figure 3 (a) shows significantly increasing absorbance with an increase in the content of *hb* -PLLA101. This indicates that short branched PLLA (*hb*-PLLA101) has lower degree of miscibility with l-PLLA matrix due to its lower l-PLLA/PG compositions in the chain. The increase in the branched structure composition, therefore, leads to lower transparency. l-PLLA/ hb -PLLA501 shows the trend of absorbance values like l-PLLA/ *hb*-PLLA101, but their values are slightly different (Figure 3(b)). This is due to the higher l-PLLA/PG content in the chain, which leads to closer solubility values of the branched structure and the PLLA matrix. In Figure 4, absorbance value increases due to increasing length of branch chain. This occur from distribution ability of large size of branch structure. Therefore, size and content of branch structure play the important role in miscibility that result in the optical transparency of blends

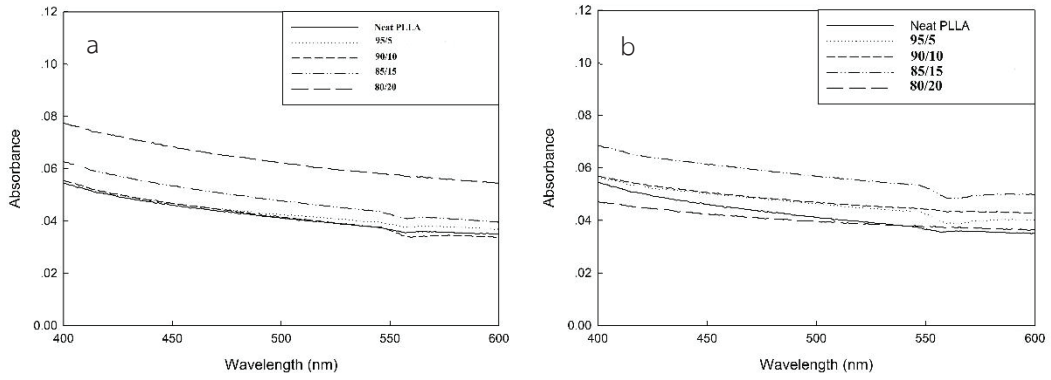

Figure 3 Absorbance of l-PLLA/*hb*-PLLA101 (a) and l-PLLA/*hb*-PLLA501 (b) varied the content of branched PLLA at the wavelength 400-600 nm.

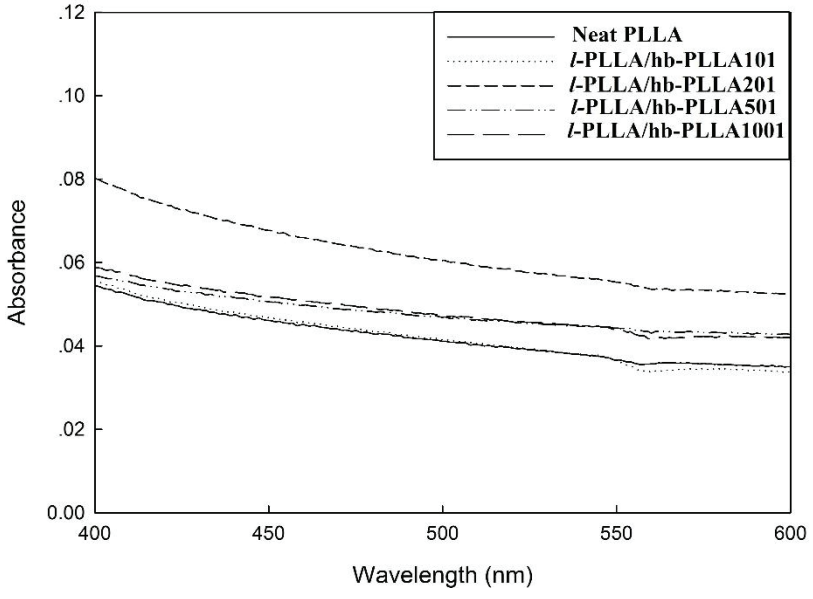

Figure 4 Absorbance of PLLA/*hb*-PLLA varied the branch chain length at the wavelength 400-600 nm.

Conclusions

Hyper branched PLLA is synthesized by bulk polymerization of LLA using polyglycidol as a macro-initiator. The copolymers are blended with l-PLLA, in which a complete miscible blend system is obtained. Upon introducing of *hb*-PLLAs, it is observed that crystallinity of the blends increase, as the branch structured act as a nucleate agent inducing crystallization of l-PLLA matrix. Toughness of PLLA/*hb*-PLLA501 (90/10) shows the highest value and other mechanical properties; tensile strength,

Young's modulus and elongation at break. This reflect an influence of an optimum blend ratio on the improvement of blends mechanical properties. The addition of *hb*-PLLAs also play an important role in rheological properties of the blends, without affecting their optical transparency. Given these properties and their biocompatibility, the blends can be used in biomedical applications.

Acknowledgement

This work was supported by Faculty of Science and Tecnology, Muban Chom Bueng Rajabhat University.

References

Ajioka, M., Enomoto, K., Suzuki, K., & Yamaguchi, A. (1995). Basic properties of polylactic acid produced by the direct condensation polymerization of lactic acid. **Bulletin of the Chemical Society of Japan,** 68(8), 2125-2131.

Atkinson, J. L., & Vyazovkin, S. (2012). Thermal Properties and Degradation Behavior of Linear and Branched Poly (L-lactide) s and Poly (L-lactide-co-glycolide) s. **Macromolecular Chemistry and Physics,** 213(9), 924-936.

Cabral, H., Miyata, K., Osada, K., & Kataoka, K. (2018). Block copolymer micelles in nanomedicine applications. **Chemical reviews,** 118(14), 6844-6892.

Cai, Q., Zhao, Y., Bei, J., Xi, F., & Wang, S. (2003). Synthesis and properties of star-shaped polylactide attached to poly (amidoamine) dendrimer. **Biomacromolecules,** 4(3), 828-834.

Choi, Y. K., Bae, Y. H., & Kim, S. W. (1998). Star-shaped poly (ether– ester) block copolymers: synthesis, characterization, and their physical properties. **Macromolecules,** 31(25), 8766-8774.

Fan, Y., Nishida, H., Shirai, Y., Tokiwa, Y., & Endo, T. (2004). Thermal degradation behaviour of poly (lactic acid) stereocomplex. **polymer Degradation and Stability,** 86(2), 197-208.

Kainthan, R. K., Janzen, J., Levin, E., Devine, D. V., & Brooks, D. E. (2006). Biocompatibility testing of branched and linear polyglycidol. **Biomacromolecules,** 7(3), 703-709.

Michalski, A., Brzezinski, M., Lapienis, G., & Biela, T. (2019). Star-shaped and branched polylactides: Synthesis, characterization, and properties. **Progress in Polymer Science,** 89, 159-212.

Ormiston, J. A., & Serruys, P. W. (2009). Bioabsorbable coronary stents. Circulation: Cardiovascular Interventions, 2(3), 255-260.

Ouchi, T., Ichimura, S., & Ohya, Y. (2006). Synthesis of branched poly (lactide) using polyglycidol and thermal, mechanical properties of its solution-cast film. **Polymer,** 47(1), 429-434.

Petchsuk, A., Buchathip, S., Supmak, W., Opaprakasit, M., & Opaprakasit, P. (2014). Preparation and properties of multi-branched poly(D-lactide) derived from polyglycidol and its stereocomplex blends. **Express Polymer Letters,** 8(10), 779-789.

Phuphuak, Y., & Chirachanchai, S. (2013). Simple preparation of multi-branched poly (l-lactic acid) and its role as nucleating agent for poly (lactic acid). **Polymer,** 54(2), 572-582.

Pistel, K. F., Bittner, B., Koll, H., Winter, G., & Kissel, T. (1999). Biodegradable recombinant human erythropoietin loaded microspheres prepared from linear and star-branched block copolymers: Influence of encapsulation technique and polymer composition on particle characteristics. **Journal of Controlled release,** 59(3), 309-325.

Rasal, R. M., Janorkar, A. V., & Hirt, D. E. (2010). Poly (lactic acid) modifications. **Progress in polymer science,** 35(3), 338-356.

Rosli, N. A., Karamanlioglu, M., Kargarzadeh, H., & Ahmad, I. (2021). Comprehensive exploration of natural degradation of poly (lactic acid) blends in various degradation media: A review. International journal of biological **macromolecules.**

Salaam, L. E., Dean, D., & Bray, T. L. (2006). In vitro degradation behavior of biodegradable 4-star micelles. **Polymer,** 47(1), 310-318.

Shibata, M., Inoue, Y., & Miyoshi, M. (2006). Mechanical properties, morphology, and crystallization behavior of blends of poly (L-lactide) with poly (butylene succinate-co-L-lactate) and poly (butylene succinate). **Polymer,** 47(10), 3557-3564.

Tuominen, J., Kylmä, J., Kapanen, A., Venelampi, O., Itävaara, M., & Seppälä, J. (2002). Biodegradation of lactic acid based polymers under controlled composting conditions and evaluation of the ecotoxicological impact. **Biomacromolecules,** 3(3), 445-455.

Uurto, I., Mikkonen, J., Parkkinen, J., Keski-Nisula, L., Nevalainen, T., Kellomäki, M., ... & Salenius, J. P. (2005). Drug-eluting biodegradable poly-D/L-lactic acid vascular stents: an experimental pilot study. **Journal of Endovascular Therapy,** 12(3), 371-379.

Xu, X., Lu, H., Luo, G., Kang, X., & Luo, Y. (2021). Theoretical insight into the opposite redox activity of iron complexes toward the ring opening polymerization of lactide and epoxide. **Inorganic Chemistry Frontiers,** 8(4), 1005-1014.